THE JOURNAL OF PHYSICAL CHEMISTRY C

Article

pubs.acs.org/JPCC

Unusual Stability and Activity of DI-Pd19 Clusters for O_2 Dissociation

Zongxian Yang,*[,†] Yanxing Zhang,[†] Zhaoming Fu,[†] and Ruqian Wu*[,‡]

[†]College of Physics and Information Engineering, Henan Normal University, Xinxiang, Henan 453007, People's Republic of China

[‡]Department of Physics and Astronomy, University of California, Irvine, California 92697-4575, United States

ABSTRACT: Density functional calculations and ab initio molecular dynamics simulations are performed to investigate adsorption and dissociation of O_2 molecules on the DI (double icosahedron) Pd19 nanocluster. Exceptionally high activity is found for oxygen bond cleavage over its waist region, with an energy barrier of only 0.06 eV and a reaction time of 0.5 ps. This stems from the availability of valley-like Pd_4 ensembles and the large weights of LUMO and HOMO. Moreover, this cluster is highly stable in reaction conditions up to 500 K, so it can be a good candidate for the development of excellent nanocatalysts.

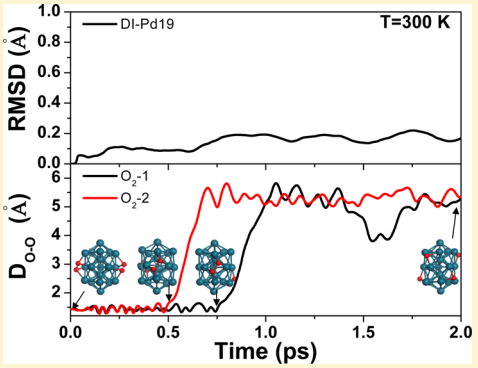

1. INTRODUCTION

The dissociation of O_2 on metal surfaces or clusters is a crucial reaction step in many chemical processes, from low-temperature water gas shift, and oxidation of CO, to more complex oxygen reduction reactions (ORRs).[1−5] The interaction between O_2 and Pd surfaces has been an attractive research topic for years,[6−10] and recent attention mainly focused on Pd stepped surfaces that are typically more active than flat surfaces due to the change of electronic and geometric features.[11,12] Interestingly, Lahti et al.[10] show that the step microfacets of Pd(211) are very active, on which the dissociation of O_2 molecules occurs at room temperature, and they attributed the activity enhancement to the formation of valley-like structures on the microfacets near the step edge. One important feature of this valley-like structure is the ensemble of four Pd atoms that may easily trap and cleave O_2 molecules. However, the density of these active ensembles is very low since high-index step surfaces are less stable than the low-index surfaces.

Small subnanometer (less than 20 atoms) clusters are catalytically active[13,14] and can be used as a building block for nanostructures. Using the many-body Gupta potential along with the genetic algorithm for the structural optimization, Borbón-González et al.[15] showed that a nanocluster in the double icosahedral (DI) geometry is the lowest-energy isomer of Pd19 (i.e., the Pd cluster with 19 atoms). Interestingly, each DI-Pd19 cluster provides five valley-like microstructures in its waist region, so these clusters can serve as good alternatives for Pd stepped surfaces for catalysis. However, most nanoclusters with less than 20 atoms are known to be vulnerable in actual reaction conditions.[16,17] Therefore, it is important to investigate the stability of DI-Pd19 clusters with the presence of O_2 molecules or oxygen adatoms.

In this paper, we demonstrate that the valley-like ensembles on the DI-Pd19 clusters are indeed extremely active for the dissociation of oxygen molecules. Using static and molecular dynamics simulations based on the density functional theory (DFT), we also show that DI-Pd19 nanoclusters are stable under the adsorption of oxygen molecules or atoms at 300 K or even higher temperature (500 K). Ab initio molecular dynamics simulations indicate that O_2 dissociates within 1 ps on the waist of the DI-Pd19 cluster. Our results indicate a credible possibility to develop these nanoclusters as efficient catalysts for various reactions.

2. MODEL AND CALCULATION

Spin-polarized calculations are performed using the Vienna Ab-initio Simulation Package (VASP).[18,19] The 4d5s of Pd and 2s2p of oxygen are treated as valence electrons, while the ionic cores are represented by the projector augmented wave (PAW) potentials.[20] The exchange and correlation interactions among electrons are described at the level of the generalized gradient approximation (GGA), using the Perdew−Burke−Ernzerhof (PBE) formula.[21] The Gaussian smearing[22] method with a half-width of 0.2 eV is employed to accelerate convergence of electron densities. The Kohn−Sham orbitals are expanded using plane waves with a well-converged energy cutoff of 400 eV. The DI-Pd19 cluster is placed in an 18.0 × 18.0 × 18.0 Å cubic supercell in order to ensure a sufficient separation between the periodic images. Since the Brillouin zone (BZ) is extremely small, only the Γ point is used to sample the BZ. All atoms are fully relaxed according to the calculated atomic forces, with a criterion that requires energies and forces to converge to better than 1.0×10^{-5} eV/atom and 0.01 eV/Å, respectively. Ab initio molecular dynamics calculations are

Received: June 29, 2012
Revised: August 6, 2012
Published: August 24, 2012

   dx.doi.org/10.1021/jp306454q | J. Phys. Chem. C 2012, 116, 19586−19589

performed with the time interval of 1 fs for motions at either 300 or 500 K using the Nose thermostat.[23]

3. RESULTS AND DISCUSSION

We first optimize the geometries of Pd19 clusters and find that they indeed prefer the DI-type shape with the *D5h* symmetry. Interestingly, the optimized DI-Pd19 cluster is magnetic, with a sizable magnetic moment, 5.43 μ_B, which is very close to Aguilera-Granja's results (6.08 μ_B).[24] This is not surprising since Pd is known to be an "almost magnetic" element in various environments. Therefore, patterned DI-Pd19 clusters on inert substrates may also be used for other technologies, such as magnetic recording and information processing. The DI-Pd19 cluster has three different (111) facets, marked by yellow, red, and blue triangles in Figure 1a. The valley-like

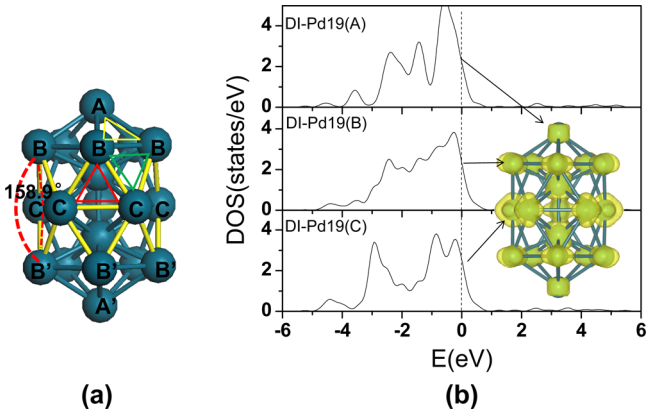

Figure 1. Structural configurations of DI-Pd19 (a), and the local density of states (LDOS) of a Pd atom on the DI-Pd19 cluster (b). Three kinds of nonequivalent Pd atoms in (a) are labeled as A, B, and C. The wave function in the energy range of [−0.05 to 0.05] eV of the Pd19 cluster is shown as an inset in (b).

structure of four Pd atoms in its waist, a buckled rhombus with a folding angle of 158.9° between two adjacent (111) facets, is denoted as BCCB′. Ten (111) facets belong to this special group, so its area ratio is significant. The wave functions of states around the Fermi level of DI-Pd19 in the inset of Figure 1b show that they mainly distribute around its waist, suggesting the activity in this region. According to their different environments, we separate surface atoms of the DI-Pd19 cluster into three categories, namely, A (A′), B (B′), and C, as denoted in Figure 1a. Curves of their local density of states (LDOS) are given in Figure 1b. We find a simple correlation between the d-band center (ε_d) away from the Fermi level and the coordination number (CN)[25] of these Pd atoms. Explicitly, the sequence of their coordination numbers is C > A or B and, accordingly, values of ε_d are −1.67 eV for C and −1.36 (−1.48 eV) for A (B). Since it is accepted that a shallower d-band center indicates stronger activity, individual A- or B-type Pd atoms on DI-Pd19 should be active toward adsorbates.

Nevertheless, we want to emphasize that the local "activity" of individual surface atoms has no direct correlation with the catalytic performance since the latter relies on activation energies of bond cleavage rather than binding energies of reactants. Here, we tackle the catalysis issues by studying the adsorption and dissociation of O_2 on the DI-Pd19 cluster on different sites. The stability of different adsorption geometries is described by the adsorption energy

$$E_{ads} = E_{O_2} + E_{Pd} - E_{O_2/Pd} \quad (1)$$

where E_{O_2} is the energy of an O_2 molecule in its gas-phase; $E_{O_2/Pd}$ and E_{Pd} are the total energies of the DI-Pd19 cluster with and without O_2, respectively. Results of E_{ads}, O−O bond length, and Bader charge of the O_2 molecule[26] are listed in Table 1. We

Table 1. Adsorption Properties of O_2 on the DI-Pd19[a]

site	E_{ads} (eV)	d_{O-O} (Å)	N_{chg} (e)
thb1	1.57	1.366	0.71
thb2	1.49	1.367	0.71
thb3	1.28	1.376	0.72
thb4	1.48	1.382	0.73
thb5	1.19	1.373	0.72
tbt1	1.51	1.340	0.63
tbt2	1.39	1.345	0.61
tbt3	1.36	1.345	0.59
bhb1	1.50	1.441	0.84

[a] d_{O-O}, the bond length of O_2 in Å; E_{ads}, the adsorption energy of O_2 in eV; N_{chg}, the number of electrons gained by O_2 from the substrates.

set many initial adsorption configurations for O_2/DI-Pd19, as depicted in Figure 2. The adsorption energies of several

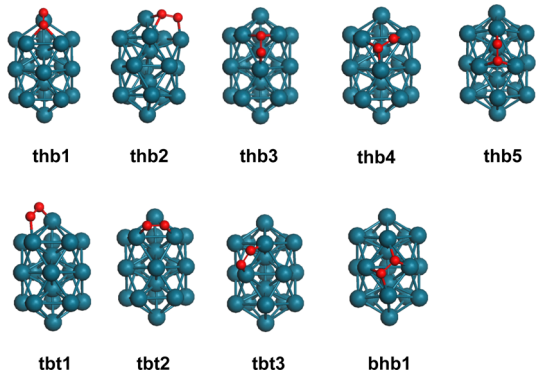

Figure 2. Initial O_2 molecule adsorption configurations on the DI-Pd19 cluster.

configurations, for example, thb1, thb4, tbt1, and bhb1, are in a narrow range: 1.48−1.57 eV. This indicates that O_2 may take these adsorption geometries with almost equal chances at room temperature. It is interesting to note that the O−O bond length expands to 1.441 Å in the bhb1 configuration over the waist of DI-Pd19. This is much longer than the corresponding values in the free O_2 molecule (1.25 Å) and also in the other geometries (1.34−1.38 Å). Therefore, the O_2 molecule is already somewhat activated in the bhb1 configuration for the dissociation step. We notice that each O_2 molecule draws 0.84 electrons from Pd atoms in this configuration, due to the availability of HOMO/LUMO in the waist region, as shown in the inset of Figure 1b. Since these additional electrons occupy the antibonding $2\pi^*$ states, charge transfer to O_2 weakens the O−O bond. The valley-like ensemble has four Pd atoms near O_2, so the energy cost by stretching the O−O bond is compensated by the enhanced O−Pd interaction.

To directly appreciate the benefit of having the valley-like ensembles on the surface, we now calculate the activation energies (E_a) for O−O bond breaking, starting from different optimized adsorption geometries. The climbing image nudged elastic band method (CI-NEB)[27] is adopted to identify reaction

dx.doi.org/10.1021/jp306454q | J. Phys. Chem. C 2012, 116, 19586−19589

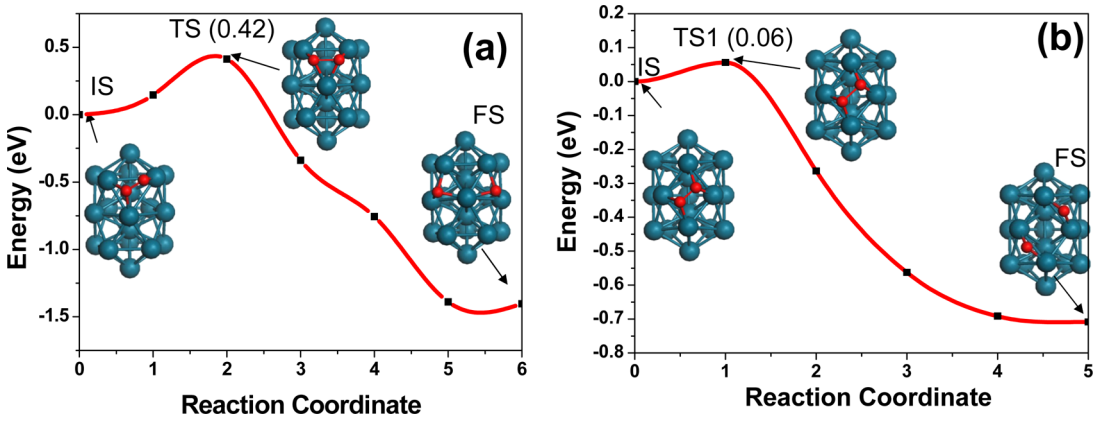

Figure 3. The two dissociation paths of O_2 on the Pd19 surface: (a) thb4 → 2hcp and (b) bhb1 → 2bri (with a bare cap region).

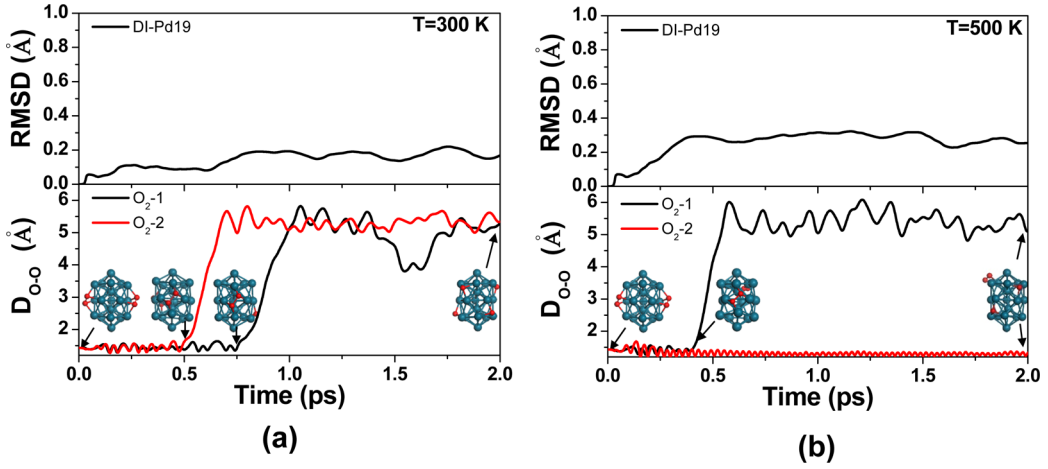

Figure 4. MD simulation of the bhb1 configuration (but here with two adsorbed O_2 molecules) for 2 ps with a time step of 1 fs at 300 K (a) and 500 K (b) for the evolvements of O−O distance (D_{O-O}) and the root-mean-square of coordinate deviations (RMSD) of Pd atoms. Snapshots of configurations for some typical points are shown in the figures.

paths and transition states, with a spring constant between adjacent images of 5.0 eV/Å. The activation energies are calculated from total energies of the initial and transition states (E_b^{IS} and E_b^{TS}) as

$$E_a = E_b^{TS} - E_b^{IS} \tag{2}$$

High activation energies are observed for O_2 dissociation over the two caps of the Pd19 cluster; for example, E_a = 0.75 eV for the thb2 → 2hcp reaction path. Therefore, we may conclude that the caps of DI-Pd19 are "inactive" toward catalyzing O_2 dissociation. It is striking that E_a is significantly reduced for O_2 dissociation over the waist region: to 0.42 eV or even 0.06 eV along two pathways depicted in Figure 3a,b that start from the thb4 and bhb1 adsorption geometries, respectively. In particular, the transition state along the pathway bhb1 → 2bri shown in Figure 3b is not much different from the initial state, due to the charge transfer from the cluster to O_2 and also the appropriate arrangement of Pd atoms for the accommodation of two oxygen atoms. The extremely small energy barrier, 0.06 eV, suggests that O−O bonds can be spontaneously cleaved once O_2 drops near the waist of the DI-Pd19 cluster in ambient conditions. Furthermore, the weakened O−O bond can be easily broken by interactions with CO or other molecules (CO_2, NH_3, H_2O, ROH, etc.).

Finally, we investigate the structural stability of the highly active DI-Pd19 nanoclusters in actual reaction conditions. This is a nontrivial issue in nanocatalysis since Ag and Pt nanocatalysts were found to quickly lose their activity as they transform to amorphous structures under the influence of reactants.[16,28] Through the structural optimization procedures at 0 K, we find that DI-Pd19 clusters are very stable even with the presence of O_2. To see if the symmetric structure can be sustained at elevated temperature, and also to directly explore the reaction speed, we carry out ab initio molecular dynamics (MD) simulations for O_2 dissociation on the DI-Pd19 cluster at 300 and 500 K. The stability of the DI-Pd19 cluster is characterized by the root-mean-square deviations (RMSDs) of coordinates of Pd atoms away from 0 K, as displayed in Figure 1a

$$\mathrm{RMSD} = \left[\frac{1}{19}\sum_{n=1}^{19}\sum_{i=1}^{3}(x_{n,i}(t) - x_{n,i}(0))^2\right]^{1/2} \tag{3}$$

Here, $x_{n,i}(0)$ is the ith coordinate of the nth Pd atom in the optimized structure at 0 K and $x_{n,i}(t)$ represents its time-dependent evolution in molecular dynamics simulations at higher temperatures. The evolvements of the O−O distance (D_{O-O}) and RMSD are shown in Figure 4. We see that thermal equilibrium is reached within 1 ps at ambient temperatures in Figure 4a. Significantly, the RMSD at 300 K is only 0.2 Å, much smaller than the average Pd−Pd bond length in the DI-Pd19 cluster, 2.76 Å. Even at 500 K, the RMSD still remains stable

dx.doi.org/10.1021/jp306454q | J. Phys. Chem. C 2012, 116, 19586−19589

around 0.3 Å in the entire time range. It is obvious that the DI-Pd19 cluster is highly stable even under the influence of oxygen molecules at elevated temperatures. This can also be seen from the snapshots in Figure 4a,b. From the sudden jumps of O−O distances at 0.5 and 0.75 ps in Figure 4a and 0.45 ps in Figure 4b, it is obvious that oxygen molecules dissociate to oxygen atoms very rapidly around the waist of DI-Pd19. This is in good accordance with the small activation energies obtained through the CI-NEB studies. Interestingly, one O_2 molecule that drifts to the cap region maintains its molecular form to the end of our MD simulations at 500 K in Figure 4b. This confirms that the caps of DI-Pd19 are inactive for O_2 dissociation, even though the adsorption energies there are high.

4. CONCLUSIONS

In summary, our systematic density functional studies and ab initio molecular dynamics simulations revealed that the DI-Pd19 nanoclusters are exceptionally active and robust for catalyzing O_2 dissociation. The synergistic effects of four Pd atoms in the particular valley-like ensemble are crucial for the enhanced catalytic activity. With an energy barrier as shallow as 0.06 eV, oxygen dissociation occurs almost spontaneously (within about a half picosecond) over the waist region. On the contrary, the caps of the DI-Pd19 cluster are inactive. It appears to be beneficial to expand DI-Pd19 clusters with more valley-like structures on their surfaces. Experimental efforts along this direction may lead to finding effective Pd nanocatalysts for many oxidation reactions. We want to mention that O_2 remains in the singlet state in the dissociation process on Pd19, so the spin effect will not change our conclusion. This is different from the sticking behavior, as discussed previously for O_2 adsorption on other metals.[29]

AUTHOR INFORMATION

Corresponding Author

*E-mail: yzx@henannu.edu.cn (Z.Y.), wur@uci.edu (R.W.).

Notes

The authors declare no competing financial interest.

ACKNOWLEDGMENTS

This work was supported by the National Natural Science Foundation of China (Grant No. 11174070) and the Innovation Scientists and Technicians Troop Construction Projects of Henan Province, China (Grant No. 104200510014). Work at UCI was supported by the National Science Foundation under CHE-0802913 and computing time at XSEDE.

REFERENCES

(1) Conrad, H.; Ertl, G.; Küppers, J. *Surf. Sci.* **1978**, *76*, 323−342.
(2) Kolasinski, K. W.; Cemic, F.; Hasselbrink, E. *Chem. Phys. Lett.* **1994**, *219*, 113−117.
(3) Eichler, A. *Surf. Sci.* **2002**, *498*, 314−320.
(4) Zhang, C.; Hu, P. *J. Am. Chem. Soc.* **2001**, *123*, 1166−1172.
(5) Yu, T.; Odell, J. H.; Jin, M.; Xia, Y. *Chem. Commun.* **2011**, *47*, 6566−6568.
(6) Jo, M.; Kuwahara, Y.; Onchi, M.; Nishijima, M. *Chem. Phys. Lett.* **1986**, *131*, 106−111.
(7) Honkala, K.; Laasonen, K. *J. Chem. Phys.* **2001**, *115*, 2297.
(8) Eichler, A.; Mittendorfer, F.; Hafner, J. *Phys. Rev. B* **2000**, *62*, 4744−4755.
(9) Wang, Z.; Jia, X.; Wang, R. *J. Phys. Chem. A* **2004**, *108*, 5424−5430.
(10) Lahti, M.; Nivalainen, N.; Puisto, A.; Alatalo, M. *Surf. Sci.* **2007**, *601*, 3774−3777.
(11) Hammer, B.; Nørskov, J. K. *Surf. Sci.* **1995**, *343*, 211−220.
(12) Hammer, B.; Nielsen, O. H.; Nrskov, J. K. *Catal. Lett.* **1997**, *46*, 31−35.
(13) Kaden, W. E.; Wu, T.; Kunkel, W. A.; Anderson, S. L. *Science* **2009**, *326*, 826−829.
(14) Vajda, S.; Pellin, M. J.; Greeley, J. P.; Marshall, C. L.; Curtiss, L. A.; Ballentine, G. A.; Elam, J. W.; Catillon-Mucherie, S.; Redfern, P. C.; Mehmood, F. *Nat. Mater.* **2009**, *8*, 213−216.
(15) Borbón-González, D. J.; Pacheco-Contreras, R.; Posada-Amarillas, A.; Schön, J. C.; Johnston, R. L.; Montejano-Carrizales, J. M. *J. Phys. Chem. C* **2009**, *113*, 15904−15908.
(16) Kim, H. Y.; Kim, D. H.; Ryu, J. H.; Lee, H. M. *J. Phys. Chem. C* **2009**, *113*, 15559−15564.
(17) Shin, K.; Kim, D. H.; Yeo, S. C.; Lee, H. M. *Catal. Today* **2011**, *185*, 94−98.
(18) Kresse, G.; Furthmüller, J. *Comput. Mater. Sci.* **1996**, *6*, 15−50.
(19) Kresse, G.; Furthmüller, J. *Phys. Rev. B* **1996**, *54*, 11169.
(20) Kresse, G.; Joubert, D. *Phys. Rev. B* **1999**, *59*, 1758.
(21) Perdew, J. P.; Burke, K.; Ernzerhof, M. *Phys. Rev. Lett.* **1996**, *77*, 3865−3868.
(22) Methfessel, M.; Paxton, A. *Phys. Rev. B* **1989**, *40*, 3616.
(23) Nosé, S. A. *J. Chem. Phys.* **1984**, *81*, 511.
(24) Aguilera-Granja, F.; Vega, A.; Rogan, J.; Orellana, W.; García, G. *Eur. Phys. J. D* **2007**, *44*, 125−131.
(25) Hammer, B.; Nørskov, J. K. *Adv. Catal.* **2000**, *45*, 71−129.
(26) Henkelman, G.; Arnaldsson, A.; Jónsson, H. *Comput. Mater. Sci.* **2006**, *36*, 354−360.
(27) Henkelman, G.; Uberuaga, B. P.; Jónsson, H. *J. Chem. Phys.* **2000**, *113*, 9901.
(28) Sun, Y.; Zhuang, L.; Lu, J.; Hong, X.; Liu, P. *J. Am. Chem. Soc.* **2007**, *129*, 15465−15467.
(29) Behler, J.; Delley, B.; Lorenz, S.; Reuter, K.; Scheffler, M. *Phys. Rev. Lett.* **2005**, *94*, 36104.